*Int. J. Appl. Math. Comput. Sci., 2022, Vol. 32, No. 2, 185–196*
DOI: 10.34768/amcs-2022-0014

# A MULTI–MODEL BASED ADAPTIVE RECONFIGURATION CONTROL SCHEME FOR AN ELECTRO–HYDRAULIC POSITION SERVO SYSTEM

ZHAO ZHANG [a,b], ZHONG YANG [b,*], SHUCHANG LIU [b], SHUANG CHEN [c], XIAOKAI ZHANG [c]

[a]Changchun Institute of Optics, Fine Mechanics and Physics
Chinese Academy of Sciences
3888 Dongnanhu Road, Erdao District, Changchun 130033, China

[b]College of Automation Engineering
Nanjing University of Aeronautics and Astronautics
29 Jiangjun Ave., Jiangning District, Nanjing 211100, China
e-mail: YangZhong@nuaa.edu.cn

[c]Electronic Engineering Department
Aviation Key Laboratory of Science and Technology on Aero Electromechanical System Integration
33 Shuige Road, Jiangning District, Nanjing 211100, China

Reliability and safety of an electro-hydraulic position servo system (EHPSS) can be greatly reduced for potential sensor and actuator faults. This paper proposes a novel reconfiguration control (RC) scheme that combines multi-model and adaptive control to compensate for the adverse effects. Such a design includes several fixed models, one adaptive model, and one reinitialized adaptive model. Each of the models has its own independent controller that is based on a complete parametrization of the corresponding fault. A proper switching mechanism is set up to select the most appropriate controller to control the current plant. The system output can track the reference model asymptotically using the proposed method. Simulation results validate robustness and effectiveness of the proposed scheme. The main contribution is a reconfiguration control method that can handle component faults and maintain the acceptable performance of the EHPSS.

**Keywords:** fault tolerant control, electro-hydraulic position servo system, multiple models, adaptive control, reconfiguration control.

## 1. Introduction

Electro-hydraulic position servo systems (EHPSSs) combine electric and hydraulic, which includes the advantages of high control precision, fast response speed, flexible signal processing, and easy-to-realize feedback of various parameters (Manring and Fales, 2019). Also, EHPSSs play a crucial role in aerospace applications, especially in the actuation of large aircraft control surfaces and control of flight simulators (Salleh *et al*., 2015). Reliability and safety are particularly important issues in the above applications.

In designing a controller for an EHPSS, there are several important considerations. The EHPSS is vulnerable to parameter uncertainty and external disturbances, such as air mixing in oil, and internal leakage (Sharifi *et al*., 2018). Many advanced control methods have been proposed to solve this problem, such as dynamic sliding mode control (Tang and Zhang, 2011), adaptive optimal compensation control (Yao *et al*., 2010), hybrid model predictive control (Yuan *et al*., 2018), feedback linearization-based control (Mintsa *et al*., 2011), and $H_\infty$ robust control (Milic *et al*., 2010). In contrast, the tracking performance of EHPSSs has been improved. Moreover, considering high-frequency interference and sensor measurement noise, Liu *et al*. (2019) investigate a kind of low-frequency learning-based robust control strategy for EHPSSs. Wang *et al*. (2014) pay attention to parametric uncertainties of EHPSSs and develop a

*Corresponding author

nonlinear robust controller based on the back-stepping design method.

Although the control effects and anti-disturbance capabilities get stronger, less emphasis is placed on component malfunctions such as sensor failures and actuator degradation. These problems may be amplified whereby the EHPSS loses its control effectiveness. For example, in the actuation of large aircraft control surfaces once a fault occurs, it will cause discrepancies between the desired and the actual movements, which may have disastrous consequences (Yu and Jiang, 2011). How to maintain the stability and acceptable performance of the EHPSS after faults becomes an interesting and challenging topic. Therefore, it is necessary to design a control system that has the capacity of tolerating potential faults automatically. Such a system is called a fault-tolerant control (FTC) system (FTCS).

With rapid advances in control and computing technologies, and motivated by increased demands for high requirements on system performance, FTC draws constantly growing attention (Pazera *et al*., 2018; Salazar *et al*., 2020; Mejdi *et al*., 2020).

A number of suitable FTC approaches have been reported for EHPSSs. A quantitative feedback theory (QFT) based FTC design is proposed by Niksefat and Sepehri (2002; 2001) for EHPSSs to deal with the abrupt sensor failures and the incorrect supply pump pressures. In the work of Sun *et al*. (2016), a fault self-healing strategy for EHPSSs based on the immune principle is designed. Mark *et al*. (2010) developed an internal mode control (IMC) based active FTC method for an EHPSS. However, the single type of faults targeted and the large sudden changes system dynamics caused by faults make it difficult for the above FTC methods to achieve reliable control quickly and accurately.

As a popular branch of FTC, reconfiguration control (RC) is widely applied to some safety-critical systems at present, especially in the field of aerospace engineering (Calise *et al*., 2001; Shin and Kim, 2004; Jain *et al*., 2012). The main idea for RC is to use system redundancy for fault compensation. Adaptive control, for its adaptability to system parametric and environmental uncertainties, is wildly used for RC design (Jiang *et al*., 2010; Zhang *et al*., 2021; Li and Yang, 2014; Falconí *et al*., 2018). However, traditional single model based adaptive control may show slow convergence in the reconfiguration problem (Yu-Ying and Jiang, 2009). Immediately after a fault system parameters of an EHPSS may be very far from its no-fault values, resulting in large transient tracking errors. A single-model based adaptive controller may take a relatively long time to bring the faulty system close to a new operating status. The performance of the EHPSS may be seriously damaged or even uncontrollable. It makes the related reconfiguration problem highly challenging.

In this paper, the problem of designing a reconfiguration scheme for EHPSSs is addressed using multi-model based adaptive control (MMAC). Each model in the multi-model set can match a type of fault, and the closest model can be chosen to describe the current fault system. A predictable fault parameter region is completely covered. Multiple model adaptive estimation methods are introduced to compensate for sensor and actuator failures in aircraft flight control systems by Maybeck (1999). Chen *et al*. (2014) proposed a reconfiguration control scheme for a quadrotor with actuator faults via adaptive control and combined multiple models. Tan *et al*. (2012) pay attention to the control of near-space vehicles and apply multiple-model based adaptive control method to compensate uncertain failures. Other RC researches based on multiple models have also produced good results (Ahmadian *et al*., 2015; Ciliz and Tuncay, 2005; Sofianos and Boutalis, 2016; Tan *et al*., 2014).

Motivated by the above observations, in this work, an MMAC based reconfiguration control scheme for EHPSSs is proposed to compensate for the adverse effects of failures and faults. It should be underlined that the term failure is used here as a permanent inability of the system to perform a given action, while a fault means degradation of a component from an acceptable range of operation. Mathematical models of EHPSSs are established based on the physical constitution and working principle. A fault-free EHPSS is introduced as the reference model so that the tracking performance is more in line with the actual situation. A reconfiguration control law is designed and its stability is proved. It is worth mentioning that the technique proposed in this paper is different from the one presented by Yu-Ying and Jiang (2009), where the multiple model set consists of adaptive models only. This work introduces several fixed models to track the system fast and an adaptive model to improve the system transient performance. Since the adaptive model is very sensitive to the initial parameters, a large error may cause slow convergence. Hence, a reinitialized adaptive model is designed for the EHPSS. It cannot only reduce the convergence time, but also decrease the number of fixed models, which in turn reduces the complexity of the algorithm and shows potential for a variety of engineering applications.

In summary, the contributions of this paper are highlighted as follows:

(i) mathematical models of EHPSSs with actuator and sensor faults are developed;

(ii) a reconfiguration control law based on model-following direct adaptive control is proposed to compensate for the adverse effects;

(iii) a multiple model set consisting of several fixed and adaptive models is designed to improve the transient

performance;

(iv) a reinitialized adaptive model is introduced to reduce the convergence time and avoid heavy computations;

(v) a proper switching scheme is set up to select the most appropriate controller to control the current plant.

The paper is organized as follows. Five subsections together form Section 2, and they introduce mathematical models of individual EHPSS components. In Section 3, reconfiguration control law is designed, followed by the proof of its stability. The fixed model design, the adaptive model design, the reinitialized adaptive model design, and the switching mechanism are presented in the four consecutive subsections of Section 4. Simulation results are presented in four cases to demonstrate the merits of the proposed method in Section 5, and conclusions are drawn in Section 6.

## 2. Mathematic models of the EHPSS

The main objective of this section is to establish fault-free and fault mathematical models for the EHPSS. The fault types are mainly the actuator loss of effectiveness and the sensor gain drift, which are typical faults of control systems.

**2.1. Composition of the EHPSS.** The closed-loop structure of the EHPSS is shown in Fig. 1 and consists of a controller, a servo amplifier, an electro-hydraulic servo valve, a hydraulic cylinder, a displacement sensor and a load. In order to formulate the problem, their mathematic models are established as follows.

**2.2. Mathematic model of a hydraulic cylinder.** The structure of the hydraulic cylinder in this paper is shown in Fig. 2. A hydraulic cylinder, an electro-hydraulic servo valve, and a load are marked with dotted lines, respectively. The specific characteristics and behavior of the hydraulic cylinder have been introduced by Manring and Fales (2019). The dynamic characteristics of the hydraulic cylinder are described by the following equations (Ma, 2003; Wang, 2017).

The flow equation of the servo valve is

$$Q_L = C_d \omega x_v \sqrt{\frac{P_s - P_L \text{sign}(x_v)}{\rho}}, \tag{1}$$

where $Q_L$ is the servo valve flow rate, $C_d$ is the flow coefficient of the servo valve, $\omega$ is the area gradient of the servo valve, $P_s$ is the oil source pressure of the system relative to the return pressure $P_r$, $P_L$=$P_1$ $-$ $P_2$ is the load pressure of the system, $x_v$ is the servo valve spool displacement, $\rho$ is the density of hydraulic oil.

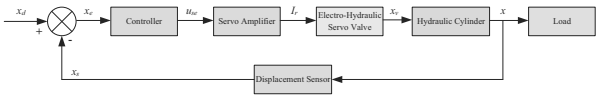


Fig. 1. Block diagram of the EHPSS.

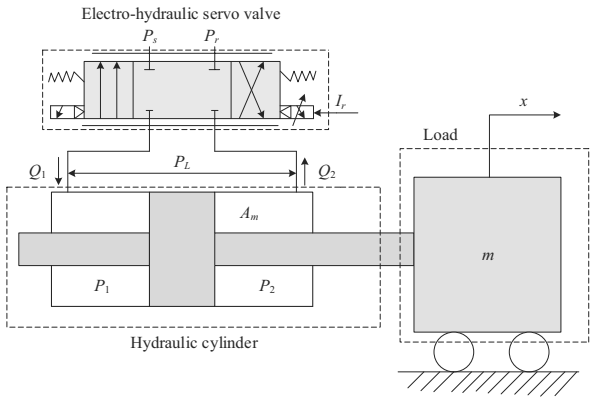


Fig. 2. Schematic diagram of a valve-controlled hydraulic cylinder.

The flow equation can be linearized as

$$Q_L = K_q x_v - K_c P_L, \tag{2}$$

where $K_q$ is the flow rate gain of the servo valve, $K_c$ is the coefficient of the flow rate to pressure of the servo valve.

The flow continuity equation of the hydraulic cylinder, with the extravasation of hydraulic oil is neglected,

$$Q_L = A_h \dot{x} + C_{tp} P_L + \frac{V_t}{4\beta_e} \dot{P}_L, \tag{3}$$

where $x$ is the piston displacement of the hydraulic cylinder, $A_h$ is the piston equivalent action area of the hydraulic cylinder, $C_{tp}$ is the leakage coefficient of the hydraulic cylinder, $V_t$ is the compression volume of the hydraulic cylinder, $\beta_e$ is the bulk elastic modulus of the hydraulic oil.

The force balance equation for the hydraulic cylinder and load is as follows:

$$A_h P_L = m\ddot{x} + B_v \dot{x} + kx + F_L, \tag{4}$$

where $m$ is the load mass, $B_v$ is the viscous damping of load, $k$ is the load spring stiffness acting on piston, $F_L$ is the external load force acting on the piston.

According to Eqns.(1)–(4), the state-space equation of the hydraulic cylinder can be obtained by eliminating

the intermediate variable,

$$\begin{bmatrix}\dddot{x}\\ \ddot{x}\\ \dot{x}\end{bmatrix} = \begin{bmatrix}\frac{4\beta_e K_{ce}+B_v V_t}{mV_t} & \frac{KV_t+4\beta_e A_h^2+4\beta_e B_v K_{ce}}{mV_t} & \frac{4\beta_e k K_{ce}}{mV_t}\\ 1 & 0 & 0\\ 0 & 1 & 0\end{bmatrix}\begin{bmatrix}\ddot{x}\\ \dot{x}\\ x\end{bmatrix} + \begin{bmatrix}-\frac{1}{m} & -\frac{4\beta_e K_{ce}}{mV_t} & \frac{4\beta_e K_q A_h}{mV_t}\\ 0 & 0 & 0\\ 0 & 0 & 0\end{bmatrix}\begin{bmatrix}\dot{F}_L\\ F_L\\ x_v\end{bmatrix}, \tag{5}$$

where $K_{ce} = K_c + C_{tp}$ is the total factor of the flow rate to pressure.

In addition, to obtain an accurate mathematical model, the influence of the elastic load and the external interference force should be neglected (Si *et al*., 2020). Since $K_{ce}B_v \ll A_h^2$, Eqn.(5) can be simplified as follows:

$$\begin{bmatrix}\dddot{x}\\ \ddot{x}\\ \dot{x}\end{bmatrix} = \begin{bmatrix}-2\zeta_h\omega_h & -\omega_h^2 & 0\\ 1 & 0 & 0\\ 0 & 1 & 0\end{bmatrix}\begin{bmatrix}\ddot{x}\\ \dot{x}\\ x\end{bmatrix} + \begin{bmatrix}\frac{K_q\omega_h^2}{A_h}\\ 0\\ 0\end{bmatrix} x_v, \tag{6}$$

where

$$\omega_h = \sqrt{\frac{4\beta_e A_h^2}{mV_t}}$$

is the hydraulic natural frequency and

$$\zeta_h = \frac{K_{ce}}{A_h}\sqrt{\frac{\beta_e m}{V_t}}$$

is the hydraulic damping ratio.

**2.3. Mathematical model of an electro-hydraulic servo valve.** A servo valve can be regarded as a two-order oscillation section, while its working frequency is close to $\omega_h$. The state-space equation of an electro-hydraulic servo valve can be described as

$$\begin{bmatrix}\ddot{x}_v\\ \dot{x}_v\end{bmatrix} = \begin{bmatrix}-2\zeta_{sv}\omega_{sv} & -\omega_{sv}^2\\ 1 & 0\end{bmatrix}\begin{bmatrix}\dot{x}_v\\ x_v\end{bmatrix} + \begin{bmatrix}K_{sv}\omega_{sv}^2\\ 0\end{bmatrix} I_r, \tag{7}$$

where $I_r$ is the input current, $K_{sv}$ is the servo valve gain, $\omega_{sv}$ is the servo valve natural frequency, $\zeta_{sv}$ is the servo valve damping ratio.

The electro-hydraulic servo valve, as the actuator of the EHPSS, is inevitably subject to potential faults. Problems such as hydraulic oil mixing with air, internal leakage, and vibrations seriously affect the efficiency of the electro-hydraulic servo system. Therefore, in this paper, the loss of effectiveness (LOE) is introduced to represent typical EHPSS actuator faults. The LOE fault is characterized by a decrease in the actuator gain from its nominal value. In the case of an actuator LOE fault, the servo valve spool displacement deviates from the command output expected by the controller. In other words, we have

$$x_v' = k_{\text{LOE}} x_v \tag{8}$$

where $x_v'$ refers to the servo valve spool actual displacement, $k_{\text{LOE}}$ represents the LOE fault gain and $k_{\text{LOE}} \in (0, 1]$.

**Remark 1.** $n\%$ LOE is equivalent to the LOE fault gain $k_{\text{LOE}} = 1 - n/100$. Here $k_{\text{LOE}} = 1$ means the fault-free actuator regime.

Therefore, the mathematical model of the hydraulic cylinder can be rewritten as follows:

$$\begin{bmatrix}\dddot{x}\\ \ddot{x}\\ \dot{x}\end{bmatrix} = \begin{bmatrix}-2\zeta_h\omega_h & -\omega_h^2 & 0\\ 1 & 0 & 0\\ 0 & 1 & 0\end{bmatrix}\begin{bmatrix}\ddot{x}\\ \dot{x}\\ x\end{bmatrix} + \begin{bmatrix}\frac{K_q\omega_h^2}{A_h}\\ 0\\ 0\end{bmatrix} x_v'. \tag{9}$$

**Remark 2.** It should be noted that if the components do not always have the same characteristics as fault-free ones, it is necessary to establish a fault model. It not only clearly illustrates how to inject component faults into the system, but also provides some accurate fault models for the design of a multiple model set next.

**2.4. Mathematic model of a displacement sensor, controller and servo amplifier.** The displacement sensor equation is simplified as

$$x_s = K_f x, \tag{10}$$

where $x_s$ is the sensor measured displacement, $K_f$ is the sensor feedback gain.

Similarly to the actuator faults, typical sensor faults such as sensor gain drifts and failures can also seriously affect the system performance and even make the system uncontrollable. The sensor fault model can be described as follows:

$$x_s' = k_{\text{DFT}} x_s \tag{11}$$

where $x_s'$ is the sensor actual output, $k_{\text{DFT}}$ represents the sensor drift coefficient and $k_{\text{DFT}} \in [0, 2]$.

**Remark 3.** $k_{\text{DFT}} = 1$ means the sensor fault-free case and $k_{\text{DFT}} = 0$ means a sensor failure.

In this paper, a PI controller is used to ensure the basic tracking performance of the EHPSS, which can be described as follows:

$$u_{se} = K_p x_e + K_i \int x_e \, \mathrm{d}t \tag{12}$$

where $u_{se}$ is the controller output voltage, $K_p$ and $K_i$ are the proportional and integral gains, respectively. $x_e = x_d - x_s'$ is the error, i.e., the difference between the desired and measured displacements.

Finally, the servo amplifier equation is

$$I_r = K_a u_{se}, \tag{13}$$

where $K_a$ is the servo amplifier gain.

**2.5. Mathematical model of the EHPSS.** According to the above modeling, the mathematical model of the fault-free EHPSS can be written down as follows:

$$\begin{cases} \dot{x}(t) = Ax(t) + Bu(t) + G\omega(t), \\ y(t) = Cx(t), \end{cases} \tag{14}$$

where $x(t) \in \mathbb{R}^n$ is the state vector, $u(t) \in \mathbb{R}^m$ is the control input vector, $\omega(t)$ models an unknown external disturbance, $y(t) \in \mathbb{R}^q$ is the output vector, $A \in \mathbb{R}^{n\times n}$, $B \in \mathbb{R}^{n\times m}$, $C \in \mathbb{R}^{q\times n}$, $G \in \mathbb{R}^n$.

**Assumption 1.** The unknown external disturbance is bounded, that is, $|\omega(t)| \leq \delta_1$, where $\delta_1$ is a positive constant.

Likewise, the fault EHPSS should also be represented uniformly for the next reconfiguration controller design, the following fault system can be obtained:

$$\begin{cases} \dot{x}_p(t) = A_p x_p(t) + B_p u_p(t) + G\omega(t), \\ y_p(t) = C_p x_p(t), \end{cases} \tag{15}$$

$$\begin{cases} A_p = A + \sigma A, \\ B_p = B + \sigma B, \\ C_p = C + \sigma C, \end{cases} \tag{16}$$

where $x_p(t) \in \mathbb{R}^{n_p}$, $u_p(t) \in \mathbb{R}^{m_p}$, $y_p(t) \in \mathbb{R}^{q_p}$, $A_p \in \mathbb{R}^{n_p\times n_p}$, $B_p \in \mathbb{R}^{n_p\times m_p}$, $C_p \in \mathbb{R}^{q_p\times n_p}$, and $\{\sigma A, \sigma B, \sigma C\}$ are parameter perturbation matrices caused by the faults.

**Assumption 2.** Each element of the parameter perturbation matrices is bounded, that is,

$$\begin{aligned} &|\sigma_{Ai}| \leq \delta_{2i}, && i = 1, \ldots, n_p \times n_p, \\ &|\sigma_{Bj}| \leq \delta_{3j}, && j = 1, \ldots, n_p \times m_p, \\ &|\sigma_{Ck}| \leq \delta_{4k}, && k = 1, \ldots, q_p \times n_p, \end{aligned}$$

where $\{\sigma_{Ai}, \sigma_{Bj}, \sigma_{Ck}\}$ denote the elements of $\{\sigma A, \sigma B, \sigma C\}$ respectively, $\{\delta_{2i}, \delta_{3j}, \delta_{4k}\}$ are some positive constants.

## 3. Reconfiguration control law design

In this paper, sensor faults and actuator (electro-hydraulic servo valve) faults are two main component faults studied. When a fault occurs, the system parameters may change abruptly, which in turn causes the actual EHPSS output to not accurately track the desired output, or even diverge. In order to reconfigure the fault system and compensate for the adverse effects, a model-following direct adaptive control method is introduced. That is, the final control objective is to design a total control signal $u_p(t)$. Such a control signal can keep all the signals in the closed-loop system bounded, and make the fault system output $y_p$ track the output of a reference model $y_m$ given by:

$$\begin{cases} \dot{x}_m(t) = A_m x_m(t) + B_m r(t), \\ y_m(t) = C_m x_m(t), \end{cases} \tag{17}$$

where $x_m(t) \in \mathbb{R}^{n_m}$, $r(t) \in \mathbb{R}^{m_m}$, $y_m(t) \in \mathbb{R}^{q_m}$, $A_p \in \mathbb{R}^{n_m\times n_m}$, $B_m \in \mathbb{R}^{n_m\times m_m}$, $C_m \in \mathbb{R}^{q_m\times n_m}$.

To achieve the control objective, the following reconfiguration control law is chosen:

$$u_{ad}(t) = K_1 r(t) + K_2 x_p(t) \tag{18}$$

where $K_1 \in \mathbb{R}^{m_p\times m_p}$ and $K_2 \in \mathbb{R}^{m_p\times n_p}$ are adaptive control gains matrices.

Substituting (18) into (15), we have

$$\begin{aligned} \dot{x}_p(t) = {} & A_p x_p(t) + B_p\left[K_1 r(t) + K_2 x_p(t)\right] \\ & + G\omega(t). \end{aligned} \tag{19}$$

Defining $e_x = x_p - x_m$ as the state error vector, we have:

$$\begin{aligned} \dot{e}_x &= x_p - x_m \\ &= A_p x_p + B_p(K_1 r + K_2 x_p) + G\omega(t) \\ &\quad - A_m x_m - B_m r \\ &= (A_p + B_p K_2) x_p + (B_p K_1 - B_m) r \\ &\quad + G\omega(t) - A_m x_m \\ &= (A_p + B_p K_2 - A_m) x_p + (B_p K_1 - B_m) r \\ &\quad + G\omega(t) + A_m e. \end{aligned} \tag{20}$$

To guarantee the asymptotic convergence of $e_x$, the following matching conditions should be satisfied:

$$\begin{cases} A_p + B_p K_2 = A_m, \\ B_p K_1 = B_m, \\ G\omega(t) = B_m {K_1}^{-1} \tilde{K}_1 r + B_m {K_1}^{-1} \tilde{K}_2 x_p. \end{cases} \tag{21}$$

Substituting (21) into (20), we have

$$\dot{e}_x = A_m e + B_m K_1^{-1} \tilde{K}_1 r + B_m K_1^{-1} \tilde{K}_2 x_p, \tag{22}$$

where $\tilde{K}_1 = K_{1_0} - K_1$, $\tilde{K}_2 = K_{2_0} - K_2$.

To guarantee $\lim_{t\to\infty} e_x(t) = 0$, the following adaptive control laws are proposed:

$$\begin{cases} \dot{K}_1 = -\Gamma_1 B_m^T P e_x x_p^T, \\ \dot{K}_2 = -\Gamma_2 B_m^T P e_x r^T. \end{cases} \tag{23}$$

**Remark 4.** $\Gamma_1$ and $\Gamma_2$ should be selected according to a practical control performance criterion, such as control precision, tracking speed, transient performance after fault occurrence.

**Theorem 1.** *For plant (15), under the reconfiguration control laws (18) and (23), all closed-loop signals are bounded. Furthermore,*

$$\begin{cases} \lim\limits_{t\to\infty} e_x(t) = 0, \\ \lim\limits_{t\to\infty} e_y(t) = \lim\limits_{t\to\infty} C_p e_x(t) = 0. \end{cases} \tag{24}$$

*Proof.* Define the following Lyapunov function:

$$V = e_x^T P e_x + \operatorname{tr}\left(\tilde{K}_1^T \Gamma_1^{-1} \tilde{K}_1\right) + \operatorname{tr}\left(\tilde{K}_2^T \Gamma_2^{-1} \tilde{K}_2\right), \tag{25}$$

where $P = P^T \in \mathbb{R}^{n_p \times n_p} > 0$ satisfies

$$A_m^T P + P A_m = -Q \tag{26}$$

for any constant matrix $Q = Q^T \in \mathbb{R}^{n_p \times n_p} > 0$.

Taking the derivative of $V$ and using (23), we obtain

$$\begin{aligned} \dot{V} &= \dot{e}_x^T P e_x + e_x^T P \dot{e}_x \\ &\quad + \operatorname{tr}\left(\dot{\tilde{K}}_1^T \Gamma_1^{-1} \tilde{K}_1 + \tilde{K}_1^T \Gamma_1^{-1} \dot{\tilde{K}}_1\right) \\ &\quad + \operatorname{tr}\left(\dot{\tilde{K}}_2^T \Gamma_2^{-1} \tilde{K}_2 + \tilde{K}_2^T \Gamma_2^{-1} \dot{\tilde{K}}_2\right) \\ &= e_x^T \left(A_m^T P + P A_m\right) e_x \\ &\quad + 2 \operatorname{tr}\left(\dot{\tilde{K}}_1^T \Gamma_1^{-1} \tilde{K}_1 + r e_x^T P B_m \tilde{K}_1\right) \\ &\quad + 2 \operatorname{tr}\left(\dot{\tilde{K}}_2^T \Gamma_2^{-1} \tilde{K}_2 + x_p e_x^T P B_m \tilde{K}_2\right) \\ &= -e_x^T Q e_x + 2 \operatorname{tr}\left[\left(\dot{\tilde{K}}_1^T \Gamma_1^{-1} \tilde{K}_1 + r e_x^T P B_m \tilde{K}_1\right)\right. \\ &\quad \left. + \left(\dot{\tilde{K}}_2^T \Gamma_2^{-1} \tilde{K}_2 + x_p e_x^T P B_m \tilde{K}_2\right)\right] \\ &= -e_x^T Q e_x \le 0 \end{aligned} \tag{27}$$

Accordingly, $0 \le V(t) \le V(0)$, and then $V(t) \in L_\infty$.

Integrating (27), we obtain

$$\begin{aligned} \int_0^\infty e_x^T Q e_x \, \mathrm{d}t &= -\int_0^\infty \dot{V} \, \mathrm{d}t \\ &= V(0) - V(\infty) < \infty. \end{aligned} \tag{28}$$

Hence $e_x \in L_2, L_\infty$ and $\dot{e}_x \in L_\infty$, which implies that (22) can be ensured. ■

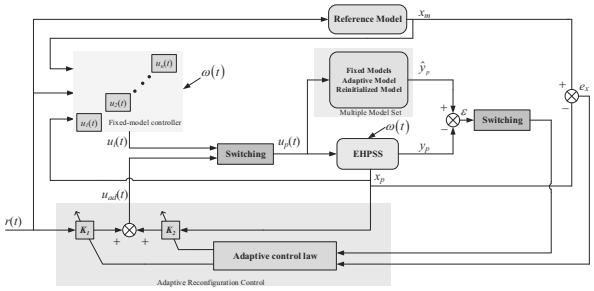


Fig. 3. Multi-model based adaptive reconfiguration control scheme.

## 4. Multiple model switching

Abrupt faults may yield large parameter jumps, and the time interval needed for an adaptive controller based on a single model to adapt to a new operating regime may be large. Over this interval, large transients may be caused that are unacceptable in practice. The desired control objective may not be achieved using a single model adaptive controller. In such a case, multiple model control is introduced to compensate the adverse effects better. This form of the proposed reconfiguration control scheme is shown in Fig. 3.

**4.1. Fixed model design.** Each fixed model corresponds to one class of fault. A fixed model is designed in the following compact form:

$$\dot{x}_{pi}(t) = \theta_i \varphi(t), \tag{29}$$

where $i = 1, 2, \ldots, n$, $\theta_i = (A_{fi}, B_{fi}, G_{fi})$ and $\varphi(t) = \left[x_p^T(t), u_p^T(t), \omega^T(t)\right]^T$.

The control objective is to design $u_p(t)$ for (29) such that the output error asymptotically converges to zero, i.e., $y_p(t) = y_m(t)$.

Next, we have

$$\begin{aligned} u_p(t) = (C_p B_p)^{-1} &\left[C_m A_m x_m(t) + C_m B_m r(t)\right. \\ &\left. - C_p A_p x_p(t) - G\omega(t)\right]. \end{aligned} \tag{30}$$

In consequence, the controller of model (29) can be obtained:

$$\begin{aligned} u_i(t) = (C_{fi} B_{fi})^{-1} &\left[C_m A_m x_m(t) + C_m B_m r(t)\right. \\ &\left. - C_{fi} A_{fi} x_p(t) - G_{fi}\omega(t)\right]. \end{aligned} \tag{31}$$

**4.2. Adaptive model design.** A bank of identification models (observers) is chosen in the following form:

$$\begin{cases} \dot{\hat{x}}_{pk} = A_p \hat{x}_{pk} + B_p \hat{u}_k + L(y_p - \hat{y}_{pk}), \\ \hat{y}_{pk} = C_p \hat{x}_{pk} \ (k = 1, 2, \ldots, n). \end{cases} \tag{32}$$

Table 1. Model parameters.

| Symbol | Description | Value |
|---|---|---|
| $K_q$ | flow rate gain of servo valve | $7.25 \times 10^{-4}\ \mathrm{m}^2/\mathrm{s}$ |
| $A_h$ | piston equivalent action area of hydraulic cylinder | $2.206 \times 10^{-4}\ \mathrm{m}^2$ |
| $m$ | load mass | $20\ \mathrm{kg}$ |
| $\beta_e$ | bulk elastic modulus of hydraulic oil | $1.5 \times 10^9\ \mathrm{Pa}$ |
| $K_{ce}$ | total factor of flow rate to pressure | $1.4 \times 10^{-12}\ \mathrm{m}^5/(\mathrm{N}\cdot\mathrm{s})$ |
| $V_t$ | compression volume of hydraulic cylinder | $1.5 \times 10^{-5}\ \mathrm{m}^3$ |
| $K_{sv}$ | servo valve gain | 16.5 |
| $\omega_{sv}$ | servo valve natural frequency | 2430rad/s |
| $\zeta_{sv}$ | servo valve damping ratio | 0.7 |
| $K_a$ | servo amplifier gain | 0.0861 |
| $K_f$ | sensor feedback gain | 12.71 |
| $K_p$ | proportional gain | 4 |
| $K_i$ | integral gain | 2 |

Define the state error as $\hat{e}_k = \hat{x}_{pk} - x_p$. Then

$$\dot{\hat{e}}_k = (A_p - LC_p)\,\dot{\hat{e}}_k + B_p\phi_k - G\omega\,(t)\,, \tag{33}$$

where $\phi_k = \hat{u}_k - u_p$, $\hat{u}_k$ is the estimate of $u_p$, and

$$\dot{\hat{u}}_k = \Gamma_3 \mathrm{Proj}\left(\hat{u}_k, -\hat{e}_x^T P_0 B_p\right), \tag{34}$$

where $\Gamma_3 \in R^+$ is the adaptive gain, 'Proj' means projection, $P_0{=}P_0^T > 0$ is a solution of the Lyapunov matrix equation

$$\begin{cases} (A_p - LC_p)^T P_0 + P_0\,(A_p - LC_p) = -Q, \\ P_0 B_p = C_p^T, \end{cases} \tag{35}$$

and $Q = Q^T > 0$.

**4.3. Switching scheme.** Define the residual error as $\varepsilon_k = \hat{y}_{pk} - y_p$. The switching performance index proposed has the form (Narendra *et al.*, 1997)

$$J_k\,(t) = a_1\|\varepsilon_k\|^2 + a_2\int_{t_o}^{t} e^{-\lambda(\tau - t_0)}\|\varepsilon_k\|^2\,\mathrm{d}\tau, \tag{36}$$

where $a_1, a_2 > 0$ can be chosen to yield a desired combination of instantaneous and long-term accuracy measures. The forgetting factor $\lambda$ determines the memory of the index during rapid switching and ensures the boundedness of $J_k\,(t)$ for bounded $\varepsilon_k$. These design parameters can be adjusted according to the given problems. The performance indices are calculated and compared at every sample interval. Then the scheme switches to (or stays at) the corresponding controller that has the minimum performance index value.

**Remark 5.** The stability of system (33) and adaptive law (34) can be ensured by the above switching scheme (Yu-Ying and Jiang, 2009). Moreover,

$$\lim_{t\to\infty} J_k\,(t) = 0, \quad \lim_{t\to\infty} \phi_k\,(t) = 0$$

are guaranteed in the case of faults (Hespanha *et al.*, 2001).

**4.4. Reinitialized adaptive model design.** When an unknown fault occurs (i.e., such a fault is not considered and designed as a fixed model), the adaptive model may take a long time to track the plant. One solution is to expand the number of fixed models to expand the fault coverage. However, too many models would lead to heavy computation (Zhai *et al.*, 2006). Hence, a reinitialized adaptive model which can update the parameters automatically with the object of the plant is introduced to improve the transient performance.

The adaptive model can be rewritten as

$$\dot{\hat{x}}_{pi}\,(t) = \hat{\theta}_i\,(t)\,\varphi\,(t)\,, \tag{37}$$

where

$$\hat{\theta}_i\,(t) = \left(\hat{A}_{fi}\,(t)\,, \hat{B}_{fi}\,(t)\,, \hat{G}_{fi}\,(t)\right),$$

and $\hat{\theta}_i\,(t_0) {=} \theta_i$.

Define $\hat{e}_i = \hat{x}_{pi} - x_p$. Based on the gradient algorithm (Sofianos and Boutalis, 2016), the parameter adaptive law for $\hat{\theta}_i\,(t)$ is chosen as follows:

$$\dot{\hat{\theta}}_i\,(t) {=} \hat{\theta}_i\,(t) - \gamma\,(t)\,\frac{\hat{e}_i\,(t)\,\varphi^T\,(t)}{1 + \varphi^T\,(t)\,\varphi\,(t)}, \tag{38}$$

where $\gamma\,(t) \in (0, 2)$is positive real number.

**Remark 6.** In essence, the reinitialized adaptive model has the same linear structure as the fixed model, while its model parameters can be changed automatically according to the parameter adaptive law (38). In this way, better model matching and satisfactory transient performance can be achieved. If there are no reinitializations after some finite time, the reinitialized adaptive model becomes a free-running adaptive model.

## 5. Simulation results

The proposed reconfiguration scheme focuses on sensor and actuator faults that are described in Section 2. Two

fixed models corresponding to two different faults (sensor drift ($k_{\text{DFT}} = 0.5$) and actuator $50\%$ LOE) are designed in the multiple model set.

The main parameters associated with the EHPSS model are given in Table 1. According to the previous modeling in Section 2, system (14) can be parameterized as follows:

$$\begin{cases} \dot{x}(t) = Ax(t) + Bu(t) + G\omega(t), \\ y(t) = Cx(t), \end{cases} \tag{39}$$

where $x(t) = [\ddot{x}, \dot{x}, x, \dot{x}_v, x_v, u_{se}] \in \mathbb{R}^6$, $y(t) = [x] \in \mathbb{R}$, $u(t) = [x_d] \in \mathbb{R}$, and

$$A = \begin{bmatrix} -2576 & -3.136 \times 10^7 & 0 \\ 1 & 0 & 0 \\ 0 & 1 & 0 \\ 0 & 0 & -4.263 \times 10^8 \\ 0 & 0 & 0 \\ 0 & 0 & -25.422 \end{bmatrix}$$

$$\begin{bmatrix} 0 & 1.031 \times 10^8 & 0 \\ 0 & 0 & 0 \\ 0 & 0 & 0 \\ -3402 & -5.905 \times 10^6 & 1.677 \times 10^7 \\ 1 & 0 & 0 \\ 0 & 0 & 0 \end{bmatrix},$$

$$B = G = \begin{bmatrix} 0 \\ 0 \\ 0 \\ 4.263 \times 10^8 \\ 0 \\ 25.42 \end{bmatrix},$$

$$C = \begin{bmatrix} 0 & 0 & 1 & 0 & 0 & 0 \end{bmatrix}.$$

The parameters of the reference model (17) are the same as (39), i.e., $A_m = A$, $B_m = B$, $C_m = C$.

For simulation, the design and simulation parameters are $\Gamma_1 = 5, \Gamma_2 = 1, \Gamma_3 = 0.001, a_1 = 100, a_2 = 1, \lambda = 0.0001, r(t) = \sin 5t, \omega(t) = 0.3 + 0.3\sin(10t)$. The effectiveness, robustness, and disturbance rejection of the proposed RC scheme are verified in the following cases:

1. $t < 0.5$ s, fault-free; $0.5\text{ s} \le t < 1.5$ s, actuator $20\%$ LOE; $1.5\text{ s} \le t < 2.5$ s, actuator $50\%$ LOE; $t \ge 2.5$ s, actuator $80\%$ LOE.

2. $t < 0.5$ s, fault-free; $0.5\text{ s} \le t < 1.5$ s, sensor drift $k_{\text{DFT}} = 0.3$; $1.5\text{ s} \le t < 2.5$ s, sensor drift $k_{\text{DFT}} = 0.5$; $2.5\text{ s} \le t < 3.5$ s, sensor drift $k_{\text{DFT}} = 0.8$; $t \ge 3.5$ s, sensor failure $k_{\text{DFT}} = 0$.

3. $t <$ ls, fault-free; $1\text{ s} \le t < 2$ s, sensor drift $k_{\text{DFT}} = 0.8$; $t \ge 2$ s, sensor drift $k_{\text{DFT}} = 0.8$ combined with actuator $50\%$ LOE .

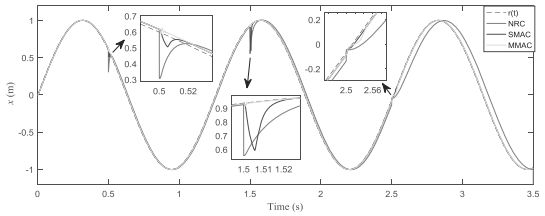


(a) system responses in Case 1

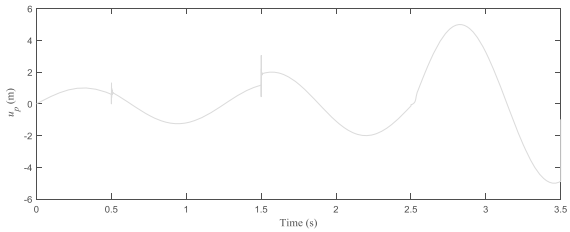


(b) control input in Case 1

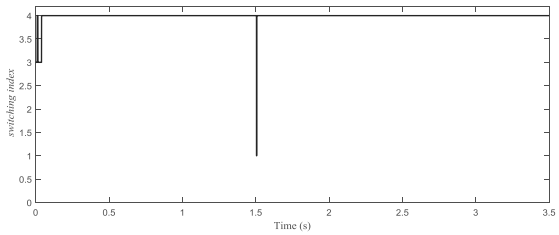


(c) switching index in Case 1

Fig. 4. System responses, control input and switching index in Case 1.

4. $t < 0.5$ s, fault-free; $0.5\text{ s} \le t < 1.5$ s, actuator $20\%$ LOE combined with $\omega(t)$ $1.5\text{ s} \le t < 2.5$ s, actuator $50\%$ LOE combined with $\omega(t)$; $t \ge 2.5$ s, actuator $80\%$ LOE combined with $\omega(t)$.

**Remark 7.** All models in the model set have been numbered:

1. fixed-model (actuator $50\%$ LOE),

2. fixed-model (sensor fault ($k_{\text{DFT}} = 0.5$)) ,

3. adaptive model,

4. preinitialized adaptive model.

**Case 1.** In Fig. 4, the fault-free system can track the reference input well. When an actuator fault occurs, a large transient error is caused in the no-reconfiguration control (NRC) system. Moreover, the response speed is greatly affected.

After applying RC, the system response has been improved obviously. Compared with single-model based adaptive control (SMAC), the transient performance of MMAC is much better, which includes faster convergence

and a smaller transient error. Besides, it clearly shows that MMAC can effectively compensate the unknown faults, which are not designed in the fixed models in advance. The robustness of the proposed method is verified. Moreover, we can see that the switching action is fast and accurate. When the actuator fault changes every time, the switching scheme chooses the most appropriate controller quickly after a short initial period of switching, and then settles down.

**Case 2.** In Fig. 5, it is clearly seen that sensor faults may have serious consequence, that is, the error between actual output and expected output are huge. In the case of a sensor constant gain drift, the transient performance of MMAC is obviously better than that of SMAC. Furthermore, for the sensor failure, SMAC causes a large amplitude oscillation, and the reconfiguration effect is very unsatisfactory. In contrast, MMAC can effectively compensate for the adverse effects of sensor failure and track the reference input well.

**Case 3.** The proposed method is introduced to reconfigure the hybrid fault, and the result is shown in Fig. 6. The advantages of MMAC such as fast convergence and a small transient error can be clearly seen. It is worth mentioning that the switching scheme always keeps on the reinitialized adaptive model, which means that the model is the best match in this case.

**Case 4.** As shown in Fig. 7, the proposed method is investigated with bounded external disturbances. The control precision of SMAC is deteriorated by the disturbance and the reconfiguration effect is unsatisfactory. Under the same disturbance, MMAC can track the reference input stably, and the control effect is basically the same as that without disturbance, which confirms the good disturbance rejection of the proposed method.

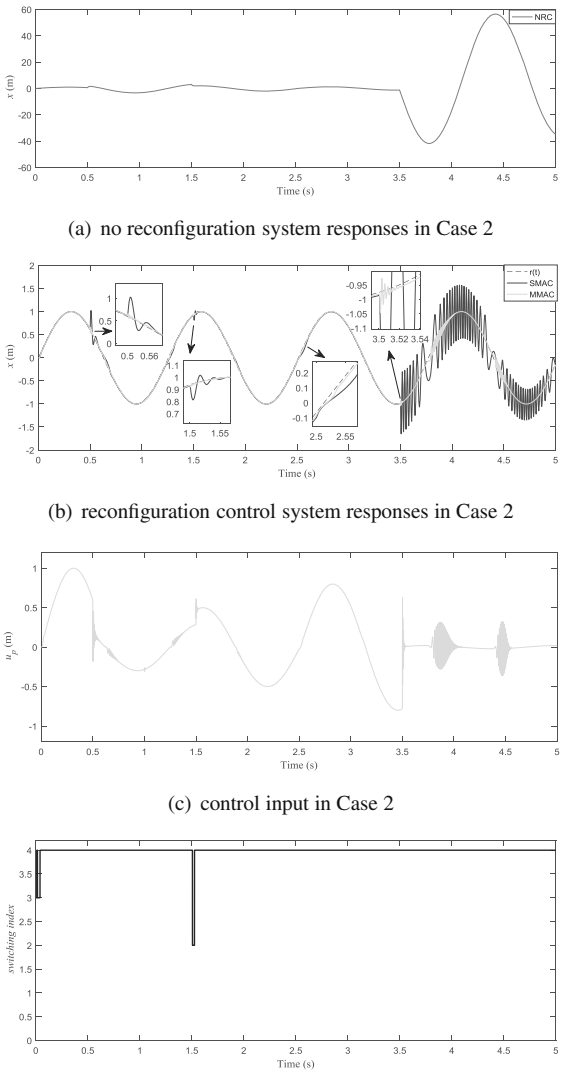


(a) no reconfiguration system responses in Case 2

(b) reconfiguration control system responses in Case 2

(c) control input in Case 2

(d) switching index in Case 2

Fig. 5. System responses, control input and switching index in Case 2.

## 6. Conclusion

This paper has demonstrated a novel reconfiguration scheme for EHPSSs, using a multiple-model based adaptive control. Mathematical models of EHPSSs are given based on the physical constitution and working principle. A reconfiguration adaptive control law is introduced to compensate the component faults. A multiple model set is proposed to cover the fault range such that the transient performance of the adaptive control can be improved. The output asymptotic tracking is guaranteed by switching the model appropriately. The reconfiguration ability and robustness of the proposed scheme have been verified through the simulation results. The main contribution of this work is the proposed reconfiguration control method that greatly enhances the reliability and safety of the EHPSS. This work makes a good start for the application of reconfiguration control in electromechanical systems.

However, the linear model-based approach ignores some nonlinear terms that may have a large impact on the fault system during the reconfiguration control process. Thus the fault tolerance of passive FTC without any fault estimation algorithm may be limited. Therefore, the future work will focus on the following points:

(i) Focus the work on the active nonlinear FTC that is more intuitive and gives more knowledge about the current status of the system.

(ii) Attempt to introduce other advance algorithms to identify the system, e.g., numerical algorithms for subspace state space system identification (N4SID).

(iii) Develop interacting multiple models to form a novel adaptive reconfiguration control method.

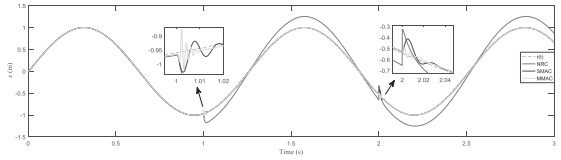


(a) system responses in Case 3

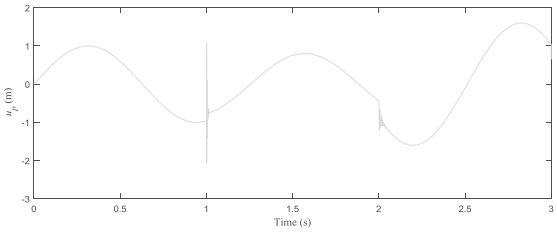


(b) control input in Case 3

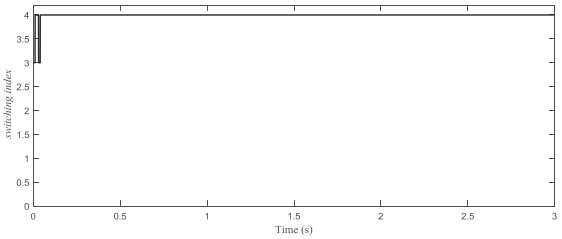


(c) switching index in Case 3

Fig. 6. System responses, control input and switching index in Case 3.

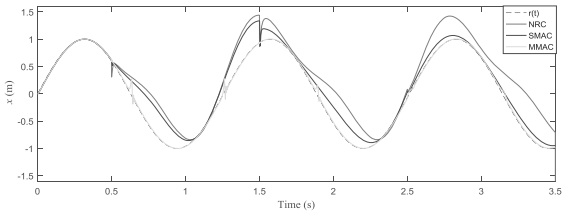


(a) system responses in Case 4

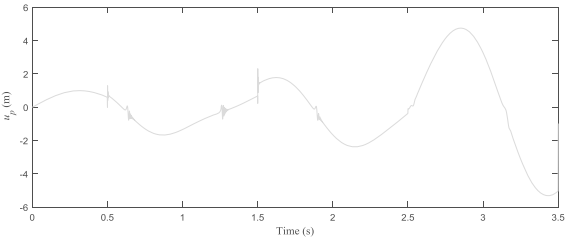


(b) control input in Case 4

Fig. 7. System responses and control inputs in Case 4.

## Acknowledgment

This study was supported by the Key Laboratory Projects of the Aeronautical Science Foundation of China (grants no. 201928052006 and 20162852031).

## References

Ahmadian, N., Khosravi, A. and Sarhadi, P. (2015). A new approach to adaptive control of multi-input multi-output systems using multiple models, *Journal of Dynamic Systems, Measurement, and Control* **137**(9): 091009.

Calise, A.J., Lee, S. and Sharma, M. (2001). Development of a reconfigurable flight control law for tailless aircraft, *Journal of Guidance, Control, and Dynamics* **24**(5): 896–902.

Chen, F., Wu, Q., Tao, G. and Jiang, B. (2014). A reconfiguration control scheme for a quadrotor helicopter via combined multiple models, *International Journal of Advanced Robotic Systems* **11**(8): 122–132.

Ciliz, M.K. and Tuncay, M. (2005). Comparative experiments with a multiple model based adaptive controller for a SCARA type direct drive manipulator, *Robotica* **23**(6): 721–729.

Falconí, G.P., Angelov, J. and Holzapfel, F. (2018). Adaptive fault-tolerant position control of a hexacopter subject to an unknown motor failure, *International Journal of Applied Mathematics and Computer Science* **28**(2): 309–321, DOI: 10.2478/amcs-2018-0022.

Hespanha, J., Liberzon, D., Stephen Morse, A., Anderson, B.D., Brinsmead, T.S. and De Bruyne, F. (2001). Multiple model adaptive control. Part 2: Switching, *International Journal of Robust and Nonlinear Control: IFAC-Affiliated Journal* **11**(5): 479–496.

Jain, T., Yamé, J.-J. and Sauter, D. (2012). Model-free reconfiguration mechanism for fault tolerance, *International Journal of Applied Mathematics and Computer Science* **22**(1): 125–137, DOI: 10.2478/v10006-012-0009-6.

Jiang, B., Guo, Y. and Shi, P. (2010). Adaptive reconfiguration scheme for flight control systems, *Proceedings of the Institution of Mechanical Engineers I: Journal of Systems and Control Engineering* **224**(6): 713–723.

Li, J.L. and Yang, G.H. (2014). Development and prospect of adaptive fault-tolerant control, *Control and Decision* **29**(11): 1921–1926.

Liu, L., Yao, J., Ma, D. and Wang, G. (2019). Low-frequency learning-based robust adaptive control for electro-hydraulic position servo system, *Acta Armamentarii* **40**(4): 737–743.

Ma, J. (2003). *Research on Intelligent Pump and Its Experiment System*, PhD thesis, Beijing University of Aeronautics and Astronautics, Beijing.

Manring, N.D. and Fales, R.C. (2019). *Hydraulic Control Systems*, John Wiley & Sons, New York.

Mark, B., Andreas, S., Marco, M. and Rolf, I. (2010). Active fault tolerant control of an electro-hydraulic servo axis with a duplex-valve-system, *IFAC Proceedings Volumes* **43**(18): 660–668.

Maybeck, P.S. (1999). Multiple model adaptive algorithms for detecting and compensating sensor and actuator/surface failures in aircraft flight control systems, *International Journal of Robust and Nonlinear Control* **9**(14): 1051–1070.

Mejdi, S., Messaoud, A. and Ben Abdennour, R. (2020). Fault tolerant multicontrollers for nonlinear systems: A real validation on a chemical process, *International Journal of Applied Mathematics and Computer Science* **30**(1): 61–74, DOI: 10.34768/amcs-2020-0005.

Milic, V., Situm, Z. and Essert, M. (2010). Robust H_infinity position control synthesis of an electro-hydraulic servo system, *ISA Transactions* **49**(4): 535–542.

Mintsa, H.A., Venugopal, R., Kenne, J.P. and Belleau, C. (2011). Feedback linearization-based position control of an electrohydraulic servo system with supply pressure uncertainty, *IEEE Transactions on Control Systems Technology* **20**(4): 1092–1099.

Narendra, S.K. and Balakrishnan, J. (1997). Adaptive control using multiple models, *IEEE Transactions on Automatic Control* **42**(2): 171–187.

Niksefat, N. and Sepehri, N. (2001). Fault tolerant control of electrohydraulic servo positioning systems, *Proceedings of the 2001 American Control Conference, Arlington, USA*, pp. 4472–4477.

Niksefat, N. and Sepehri, N. (2002). A QFT fault-tolerant control for electrohydraulic positioning systems, *IEEE Transactions on Control Systems Technology* **10**(4): 626–632.

Pazera, M., Buciakowski, M. and Witczak., M. (2018). Robust multiple sensor fault-tolerant control for dynamic non-linear systems: Application to the aerodynamical twin-rotor system, *International Journal of Applied Mathematics and Computer Science* **28**(2): 297–308, DOI: 10.2478/amcs-2018-0021.

Salazar, J.C., Sanjuan, A., Nejjari, F. and Sarrate, R. (2020). Health-aware and fault-tolerant control of an octorotor UAV system based on actuator reliability, *International Journal of Applied Mathematics and Computer Science* **30**(1): 47–59, DOI: 10.34768/amcs-2020-0004.

Salleh, S., Rahmat, M.F., Othman, S.M. and Danapalasingam, K.A. (2015). Review on modeling and controller design of hydraulic actuator systems, *International Journal on Smart Sensing & Intelligent Systems* **8**(1): 338–367.

Sharifi, S., Tivay, A., Rezaei, S.M., Zareinejad, M. and Mollaei Dariani, B. (2018). Leakage fault detection in electro-hydraulic servo systems using a nonlinear representation learning approach, *ISA Transactions* **73**: 154–164.

Shin, D.H. and Kim, Y. (2004). Reconfigurable flight control system design using adaptive neural networks, *IEEE Transactions on Control Systems Technology* **12**(1): 87–100.

Si, G., Shen, Y., Wang, J., Cao, T. and Wan, M. (2020). Active disturbance rejection control of electro-hydraulic position servo system, *Chinese Hydraulics & Pneumatics* **12**(3): 14–21.

Sofianos, N.A. and Boutalis, Y.S. (2016). Robust adaptive multiple models based fuzzy control of nonlinear systems, *Neurocomputing* **173**: 1733–1742.

Sun, W., Jian, D., Yuan, Y. and Yuan, Y. (2016). Fault simulation of electro-hydraulic servo system for fault self-healing based on immune principle, *2016 9th International Symposium on Computational Intelligence and Design (ISCID), Hangzhou, China*, pp. 136–139.

Tan, C., Tao, G. and Qi, R. (2014). An adaptive control scheme using multiple reference models, *International Journal of Adaptive Control and Signal Processing* **28**(11): 1290–1298.

Tan, C., Yao, X.and Tao, G. and Qi, R. (2012). A multiple-model based adaptive actuator failure compensation scheme for control of near-space vehicles, *IFAC Proceedings Volumes* **45**(20): 594–599.

Tang, R. and Zhang, Q. (2011). Dynamic sliding mode control scheme for electro-hydraulic position servo system, *Procedia Engineering* **24**: 28–32.

Wang, C., Shang, Y., Jiao, Z. and Han, S. (2014). Nonlinear robust control of valve controlled electro-hydraulic position servo system, *Journal of Beijing University of Aeronautics and Astronautics* **40**(12): 1736–1740.

Wang, H. (2017). *Research on an Adaptive Sliding Mode Control Strategy for Electro-Hydraulic Position Servo System*, PhD thesis, Shanghai Jiao Tong University, Shanghai.

Yao, J., Jiao, Z., Shang, Y. and Huang, C. (2010). Adaptive nonlinear optimal compensation control for electro-hydraulic load simulator, *Chinese Journal of Aeronautics* **23**(6): 101–114.

Yu, X. and Jiang, J. (2011). Hybrid fault-tolerant flight control system design against partial actuator failures, *IEEE Transactions on Control Systems Technology* **20**(4): 871–886.

Yu-Ying, G. and Jiang, B. (2009). Multiple model-based adaptive reconfiguration control for actuator fault, *Acta Automatica Sinica* **35**(11): 1452–1458.

Yuan, H.B., Na, H.C. and Kim, Y.B. (2018). System identification and robust position control for electro-hydraulic servo system using hybrid model predictive control, *Journal of Vibration and Control* **24**(18): 4145–4159.

Zhai, J., Fei, S. and Da, F. (2006). Intelligent control using multiple models based on on-line learning, *Journal of Control Theory and Applications* **4**(4): 397–401.

Zhang, Z., Yang, Z., Xiong, S., Chen, S., Liu, S. and Zhang, X. (2021). Simple adaptive control-based reconfiguration design of cabin pressure control system, *Complexity* **2021**(3): 1–16.

**Zhao Zhang** holds BS (2019) and MS (2022) degrees from the Nanjing University of Aeronautics and Astronautics. He is currently a research assistant in the Electro-Optical Countermeasures Department at the Changchun Institute of Optics, Fine Mechanics and Physics. His research interests include modeling and control of aviation electromechanical systems, adaptive control, fault tolerant control system design, and reconfiguration control technology.

**Zhong Yang** received his PhD degree in mechanical manufacture engineering from the Nanjing University of Aeronautics and Astronautics in 1998. He is currently a professor with the College of Automation Engineering, Nanjing University of Aeronautics and Astronautics. His research interests include intelligent robots, intelligent measurements and fault diagnosis, as well as machine vision and its application.

**Shuchang Liu** received her BS degree in electrical engineering from the Nanjing University of Aeronautics and Astronautics in 2020. She is currently pursuing her MS degree in the College of Automation Engineering at the Nanjing University of Aeronautics and Astronautics. Her research interest includes intelligent fault diagnosis, adaptive control, and reconfiguration control technology.

**Shuang Chen,** MS, is currently an engineer with the Electronic Engineering Department, Aviation Key Laboratory of Science and Technology on Aero Electromechanical System Integration. His research interest is in electromechanical control.

**Xiaokai Zhang,** BS, is currently a senior engineer with the Electronic Engineering Department, Aviation Key Laboratory of Science and Technology on Aero Electromechanical System Integration. His research interest is in control engineering.

Received: 24 May 2021
Revised: 15 August 2021
Accepted: 28 September 2021